PILOT PROTECTION OF ACTIVE DISTRIBUTION NETWORK BASED ON POSITIVE SEQUENCE CURRENT SELF-SYNCHRONIZATION TECHNOLOGY

You YU[1], Jingfu TIAN[2], Mingzhe SUN[3,*], Gang WANG[4], Pengfei TIAN[5], Qingzhe XI[6]

Distributed generation (DG) decreases the reliability of traditional current protection in the distribution network. Pilot protection is effective to solve this problem theoretically. But the asynchronous problem hinders its application, caused by the limited communication conditions and the inconsistent sampling times at both ends of the line. This paper proposes a self-synchronization technology of positive sequence currents (PSCs) and develops a pilot protection principle based on the similarity characteristics of the PSC fault components (PSCFCs). Without considering the capacitance-to-ground, the currents at both ends of the line are almost equal theoretically before the fault occurrence. Therefore, the self-synchronization technology calculates the currents' angle difference caused by the asynchronous problem by minimizing the differential current amplitude of normal operation. Then, it realizes the synchronization of the PSCs according to the calculated angle difference. Further, due to the ability of PSCFC against the transient resistance, this paper utilizes the PSCFCs similarity characteristics to construct a pilot protection principle distinguishing external fault and internal fault. Finally, considering the effects of various fault conditions, such as transient resistance, fault occurrence time, DG penetration, and so on, many simulations verify the higher reliability of the proposed protection principle. The protection principle ensures the power supply reliability and has certain engineering application value.

Keywords: pilot protection; fault component of positive sequence current; similarity characteristics; self-synchronization technique

1. Introduction

To solve the energy crisis and environmental pollution, distributed generation (DG) is developing rapidly worldwide [1-3]. But the traditional distribution network's structure changes due to DG's integration, resulting in the complex fault characteristics of the distribution network. Therefore, the traditional

[1] Liaoning Electric Power Company, State Grid Corporation of China, Shenyang, China
[2] Liaoning Electric Power Company, State Grid Corporation of China, Shenyang, China
[3] * School of Electrical Engineering Northeast Electric Power University, Jilin, China, corresponding e-mail: delete568djh@163.com
[4] Benxi Power Supply Company, State Grid Corporation of China, Benxi, China
[5] Liaoning Electric Power Company, State Grid Corporation of China, Shenyang, China
[6] Benxi Power Supply Company, State Grid Corporation of China, Benxi, China

current protection has the problem of insufficient reliability and sensitivity in the active distribution network. It is of great significance to propose a protection principle suitable for the active distribution network.

Many new protection principles have been proposed by relay protection scholars, which are mainly divided into the following two categories. The first category [4-13] improves the protection based on local information, automatically adjusting the protection setting value according to the system operation mode and fault type. For example, literature [10] proposes a fast current protection scheme. It can adjust the protection setting value in real-time. However, the method has high requirements for the communication conditions and intelligence level of the system. Literature [12] proposed a self-adapting positive sequence current (PSC) quick-break protection with inverter-interfaced distribution generation. Through studying the relationship between the positive sequence voltage and the PSC, a new protection setting formula is constructed. The protection can adjust the protection setting value online. However, the protection can only achieve self-adaptive adjustment if the direction elements are installed at each protection location. The second category [14-18] is pilot protection based on the double-end information of the line. However, the asynchronous problem caused by the limited communication conditions and the inconsistent sampling times at both ends of the line affects the reliability of the pilot protection significantly. To solve this problem, literature [14] proposed a protection scheme based on the current amplitude difference to avoid the influence of asynchronous problem on pilot protection. According to the unequal current amplitudes at both ends of the faulty line, the protection setting formula criterion is constructed to improve the sensitivity of protection. However, the large transition resistance may cause the refusal-operation of this protection. Literature [15] proposes a pilot protection scheme based on positive sequence impedance. According to the amplitude difference of positive sequence impedance, the protection criterion is constructed to improve the reliability and sensitivity of protection. But at the same time, this scheme has high requirements for communication conditions. Literature [16] analyses the control strategy of DG and proposes the PQ control equivalence model and the pilot protection by using voltage information. However, these protection schemes need to obtain the voltage information at the protection installation. In the current distribution network feeders, voltage transformers are generally not equipped. Therefore, the voltage information is difficult to obtain [17-18].

Due to the ability of the PSC fault component (PSCFC) against the transition resistance, this paper utilizes the similarity of PSCFCs to construct a pilot protection principle with a new self-synchronization technology. Without considering the capacitance-to-ground, the currents at both ends of the line are almost equal theoretically before the fault occurrence. Therefore, this study

proposes the self-synchronization technology which calculates the currents' angle difference caused by the asynchronous problem by minimizing the differential current amplitude before the fault occurrence. Further, according to the angle difference, the PSCs at both ends of the line realize synchronization. By taking full advantage of the amplitude and angle characteristics of PSCFC, the proposed protection principle can identify the internal fault accurately and reliably. This paper firstly analyses the characteristics of PSCFC in the active distribution network. Then, this paper proposes the PSC self-synchronization technology and constructs the protection criterion. Finally, the simulation results verify the effectiveness of the proposed protection scheme.

2. Similarity Characteristics of Fault Components in Active Distribution Network

2.1 Characteristics of PSCFC in Active Distribution Network

To study the characteristics of PSCFC, an active distribution network model is built as shown in Fig. 1. In Fig. 1, the protection scheme is configured at the circuit breaker CB*i*. After a fault occurs, due to the uncertainty of DG output, it is no longer applicable to equivalent DG by using a voltage source in series with internal impedance. Since the requirement for the low voltage ride-through capability, the output fault current of DG is related to the degree of voltage drop at the grid-connected point. At present, many studies use the voltage-controlled current source to equivalent DG [20-21]. The positive sequence fault additional sequence network is shown in Fig. 2.

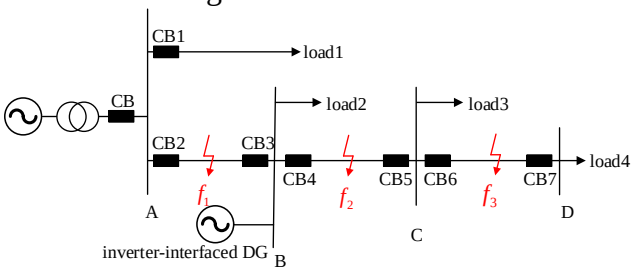

Fig. 1. 10kV active distribution network model.

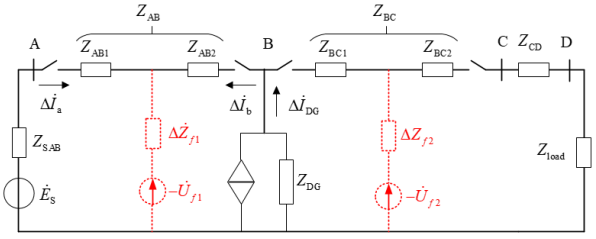

Fig. 2. Schematic diagram of positive sequence network.

In Fig. 2, Z_{AB1} and Z_{AB2} correspond to the positive sequence impedance from the fault point to the bus A and B respectively; $-\dot{U}_{f1}$ and $-\dot{U}_{f2}$ are the fault electromotive forces at the fault point; ΔZ_{f1} and ΔZ_{f2} are the additional impedance of the fault; Z_{AB}, Z_{BC} and Z_{CD} correspond to the positive sequence impedance of lines AB, BC and CD. Z_{load} is the load impedance. $\Delta\dot{I}_{\mathrm{a}}$ and $\Delta\dot{I}_{\mathrm{b}}$ are the PSCFCs at the head and end of the line respectively, whose positive direction is shown in Fig. 2. Z_{DG} is the unloading circuit used to limit the maximum short circuit current of inverter-interfaced DG (IIDG) [21]. $\Delta\dot{I}_{\mathrm{DG}}$ is the PSCFC output of DG.

According to the superposition theorem, the PSCFCs at both ends of the line for the internal faults on line AB are obtained by the combined action of the fault electromotive force and the equivalent current source of DG. Taking a three-phase short circuit as an example, the PSCFCs are shown in Equations (1) and (2).

$$\Delta\dot{I}_{\mathrm{a}} \approx \frac{\dot{U}_{f1}\cdot Z'_{\mathrm{B}} - \Delta\dot{I}_{\mathrm{DG}}\cdot\Delta Z_{f1}\cdot Z'_{\mathrm{load}}}{\Delta Z_{f1}\cdot(Z_{\mathrm{AB1}}+Z'_{\mathrm{B}}) + Z_{\mathrm{AB1}}\cdot Z'_{\mathrm{B}}} \tag{1}$$

$$\Delta\dot{I}_{\mathrm{b}} \approx \frac{\dot{U}_{f1}\cdot Z_{\mathrm{AB1}} + \Delta\dot{I}_{DG}\cdot Z'_{\mathrm{load}}\cdot(Z_{\mathrm{AB1}}+\Delta Z_{f1})}{\Delta Z_{f1}\cdot(Z_{\mathrm{AB1}}+Z'_{\mathrm{B}}) + Z_{\mathrm{AB1}}\cdot Z'_{\mathrm{B}}} \tag{2}$$

Where $Z'_{\mathrm{load}}=Z_{\mathrm{BC}}+Z_{\mathrm{CD}}+Z_{\mathrm{load}}$, $Z'_{\mathrm{B}}=Z_{\mathrm{AB2}}+Z'_{\mathrm{load}}$.

According to equations (1) and (2), the PSCFCs on both ends of the line are mainly affected by fault location, fault type and positive sequence impedance. Therefore, the protection principle based on PSCFC has the ability against transition resistance under different fault conditions.

2.2 Similarity Analysis of PSCFC

In this paper, the similarity characteristics of PSCFCs are analyzed for the BC line when the internal and external faults occur. Without considering the capacitance-to-ground, the PSCs at both ends of the line are approximately equal in normal operation. As shown in Fig. 3 (a), $\dot{I}_{\mathrm{b}}^{+}$ and $\dot{I}_{\mathrm{c}}^{+}$ are the PSCs at the head and end of the line BC respectively, x and y refer to the real part and the imaginary part of the PSC respectively. According to Fig. 3 (a), both the amplitudes and phase angles of $\dot{I}_{\mathrm{b}}^{+}$ and $\dot{I}_{\mathrm{c}}^{+}$ are almost equal.

When an external fault occurs, the PSCs at both ends of the line, $\dot{I}_{\mathrm{bE}f}^{+}$ and $\dot{I}_{\mathrm{cE}f}^{+}$, are still equal approximately. Compared with normal operation, the PSC amplitudes in the event of the external faults are larger but the phase angles are still equal, as shown in Fig 3. (a). The PSCFCs, $\Delta\dot{I}_{\mathrm{bE}f}^{+}$ and $\Delta\dot{I}_{\mathrm{cE}f}^{+}$, are calculated

and show the distinct characteristics that both the amplitudes and the phase angles are approximately equal, as shown by the phasors in blue color. According to the analysis, the PSCFCs at both ends of the line are similar in event of the external faults. When an internal fault occurs, the amplitudes and phase angles of PSCs at both ends of the line, $\dot{I}^{+}_{\mathrm{bI}f}$ and $\dot{I}^{+}_{\mathrm{cI}f}$, are different, as shown by the phasors in Fig. 3 (b). Therefore, when an internal fault occurs, the similarity of the PSCFCs at both ends of the line decreases due to the fault current.

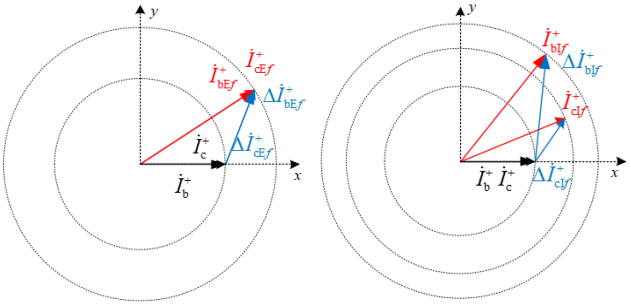

(a) (b)

Fig. 3. Schematic diagram of PSC phasors. (a) external fault. (b) internal fault.

Based on the above analysis, the similarity characteristics of PSCFCs are helpful to construct the pilot protection criterion. However, when the asynchronous problem exits, it is difficult to extract the similarity characteristics of the PSCFCs accurately. As shown in Fig. 4, the angle difference caused by the asynchronous problem is defined δ. In particular, without the consideration of the capacitance-to-ground, the angle difference δ is only related to the asynchronous problem under the event of normal operation and external faults.

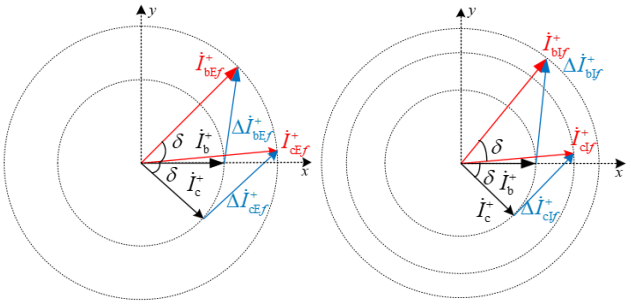

(a) (b)

Fig. 4. Schematic diagram of PSC phasors with angle difference. (a) external fault. (b) internal fault.

When an external fault occurs, due to the asynchronous problem, the similarity of PSCFCs decreases. Therefore, it is difficult to accurately distinguish external and internal faults by using PSCFCs directly. Similarly, for internal faults, the

similarity characteristics of PSCFCs are more complex due to the combined effect of the angle difference δ and the fault current.

In conclusion, due to the asynchronous problem, the similarity characteristics of PSCFCs at both ends of the line are uncertain and cannot be directly used to construct the protection criteria.

3. PSC Self-Synchronization Technology

3.1 Proposal of PSC Self-Synchronization Technology

According to the above analysis, for internal faults and external faults, the similarity of the PSCFCs is affected by asynchronous problem. Therefore, a self-synchronization technique is proposed to solve the problem. At present, the mainstream self-synchronization technology realizes self-synchronization based on the mutation characteristics. When an internal fault or external fault occurs, the mutation characteristics of PSCs at both end of the line are different due to fault current and the measurement error. So, the detected fault occurrence times at both ends of the line may be inconsistent. Therefore, the asynchronous problem has not been completely solved. Without considering the capacitance-to ground, the PSCs at both ends of the line are basically equal before the fault occurrence. The difference of PSCs in normal operation is only related to the asynchronous problem. Therefore, the PSC self-synchronization technology calculates the asynchronous angle difference by minimizing the differential current amplitude before the fault occurrence. Furthermore, the PSC self-synchronization technology corrects the PSCs after fault occurrence to realize self-synchronization.

Therefore, this paper proposes a PSC self-synchronization technology based on the current before the fault occurrence to realize the self-synchronization of the PSCs at both ends of the line.

3.2 Realization of PSC Self-Synchronization Technology

The differential current amplitude before fault occurrence is shown in Equation (3).

$$\left|\dot{I}_1-\dot{I}_2\right|=\sqrt{\left|\dot{I}_1\right|^2+\left|\dot{I}_2\right|^2-2\left|\dot{I}_1\right|\left|\dot{I}_2\right|\cos(\alpha-\beta-\delta)} \tag{3}$$

$\left|\dot{I}_1\right|$ and α are the current amplitude and phase angle at the head of the line respectively. $\left|\dot{I}_2\right|$ and β are the current amplitude and phase angle at the end of the line respectively. δ is the angle difference between $\dot{I}_1$ and $\dot{I}_2$, caused by asynchronous problem. The relationship between the angle difference δ and the differential current amplitude $\left|\dot{I}_1-\dot{I}_2\right|$ is shown in Fig. 5. When α, β and δ meet $\alpha-\beta-\delta=0$, the $\cos(\alpha-\beta-\delta)$ is the maximum and the differential current

amplitude $\left|\dot{I}_1-\dot{I}_2\right|$ is the minimum. Without considering the capacitance-to-ground, the angles α and β of PSCs at both ends of the line are basically equal, namely $\alpha-\beta\approx 0$. Therefore, with the increase of asynchronous angle δ, the differential current amplitude $\left|\dot{I}_1-\dot{I}_2\right|$ increases. Furthermore, when $\dot{I}_1$ is synchronized with $\dot{I}_2$, the differential current amplitude $\left|\dot{I}_1-\dot{I}_2\right|$ is the minimum. Therefore, the PSC self-synchronization technology calculates the current' phase angle difference caused by the asynchronous problem by minimizing the differential current amplitude $\left|\dot{I}_1-\dot{I}_2\right|$. The self-synchronization technology has been detailed as below.

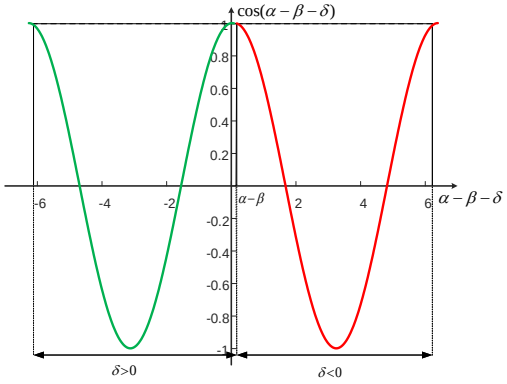

Fig. 5. Diagram of PSC angle deviation.

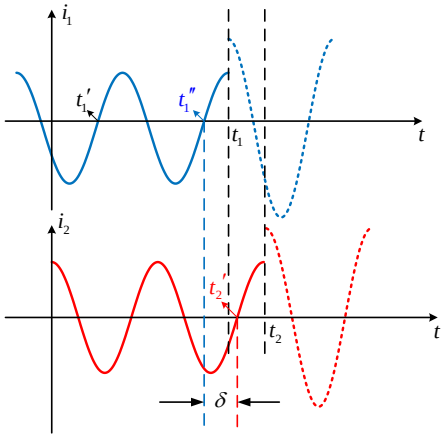

Fig. 6. Schematic diagram of PSC self-synchronization technology.

Assuming the detected current mutation times of PSCs at both ends of the line are t_1 and t_2 respectively, but which are not generally equal to the real fault occurrence time t. The angle difference caused by the asynchronous problem is δ, as shown in Fig. 6.

Firstly, a current $\dot{I}_{10}$ of normal operation is selected at a certain time t_1' for the head of the line and a current $\dot{I}_{20}$ the end of the line is preliminary determined as the synchronization current of $\dot{I}_{10}$. Specifically, the differential current amplitudes $\left|\dot{I}_{10}-\dot{I}_2\right|$ are calculated, where $\dot{I}_2$ represents any current at the end of the line of several cycles before the time t_2. Fig. 7 has shown the changes of the differential current amplitudes $\left|\dot{I}_{10}-\dot{I}_2\right|$. According to Fig. 7, the current $\dot{I}_2$ at the time t' will make $\alpha-\beta-\delta=0$ in Fig 5. Then, the time t' closest to the time t_2 is

preliminarily determined as the synchronization point of time t_1' and is denoted by t_2'. The current $\dot{I}_2$ at the time t_2' is defined as $\dot{I}_{20}$.

Secondly, this self-synchronization technology determines whether the current $\dot{I}_{20}$ is the real synchronization current of the current $\dot{I}_{10}$. Specifically, it calculates the differential current amplitudes $\left|\dot{I}_1 - \dot{I}_{20}\right|$, where $\dot{I}_1$ represents any current at the head of the line between the time t_1 and the time t_1'. If there is time t_1'' when the amplitude reaches the minimum, the time t_2' is not the real synchronization point of the time t_1' but the time t_1''. Otherwise, the time t_2' is the real synchronization point of the time t_1'. Finally, the angle difference is calculated according to t_2' and t_1' (or t_1'') to realize the self-synchronization of PSCs. With the self-synchronization technology of PSCs, the PSCFCs at both ends of the line are calculated and used to construct the pilot protection principle.

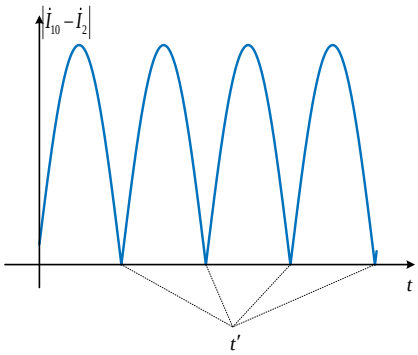

Fig. 7. Differential current amplitude between two ends of line at different time.

4. New Pilot Protection Principle of Active Distribution Network

The calculation formula of fault component is shown in equation (4).

$$\Delta\dot{I} = \dot{I}(t) - (-1)^n \dot{I}(t - n\frac{T}{2}) \tag{4}$$

$\Delta\dot{I}$ is the PSCFC of the line. $\dot{I}(t)$ is the PSC after the fault occurrence. T is the frequency period. n is an integer, such as 1, 2 or 3. In this paper, n is determined 2. Equation (4) can be simplified to equation (5).

$$\Delta\dot{I} = \dot{I}(t) - \dot{I}(t - T) \tag{5}$$

Next, the Euclidian distance is used to analyze PSCFCs similarity, as shown in equation (6).

$$D(\Delta\dot{I}_1,\Delta\dot{I}_2)=\sqrt{(X_{11}-X_{21})^2+(X_{12}-X_{22})^2} \tag{6}$$

$\Delta\dot{I}_1 = X_{11} + \mathrm{j}X_{12}$ and $\Delta\dot{I}_2 = X_{21} + \mathrm{j}X_{22}$ are fault components at the head and end of the line respectively. X_{11} and X_{21} are the real parts of fault components $\Delta\dot{I}_1$ and $\Delta\dot{I}_2$. X_{12} and X_{22} are the imaginary parts of fault components $\Delta\dot{I}_1$ and $\Delta\dot{I}_2$.

According to the above analysis, the similarity value of PSCFCs is low when an external fault occurs. When an internal fault occurs, the similarity value of PSCFCs is high. Therefore, the similarity value of PSCFCs D_{set} is used to construct the protection criterion in this paper. The selection of similarity threshold should take into account the influence of non-periodic component and system disturbance. In this paper, the similarity threshold D_{set} is set to 0.1 based on a large amount of simulation data. The similarity threshold D_{set} can be adjusted according to the operation experience and actual demand. When the PSCFCs similarity value $D(\Delta\dot{I}_1,\Delta\dot{I}_2)$ meets $D(\Delta\dot{I}_1,\Delta\dot{I}_2) > D_{set}$, it is an internal fault. Otherwise, it is an external fault.

5. Case Study

To verify the effectiveness of proposed protection principle, a simulation model shown in Fig. 8 of active distribution network in Fig. 1 is established in PSCAD. The reference capacity of system source is 100MVA and the reference voltage is 10.5kV. The line in active distribution network are overhead lines, where the lengths of the lines are 2km and the line impedance is 0.27+j0.35 Ω/km. In this paper, for the section BC, the external faults *f*1, *f*3 and the internal faults *f*2 are conducted to analyze the similarity of PSCFCs, where various fault conditions are considered sufficiently, such as DG penetration, fault type, fault location, transition resistance, load level, fault occurrence time and so on. Then, the similarity values of the faults are compared with the protection threshold D_{set} to identify the external and internal faults.

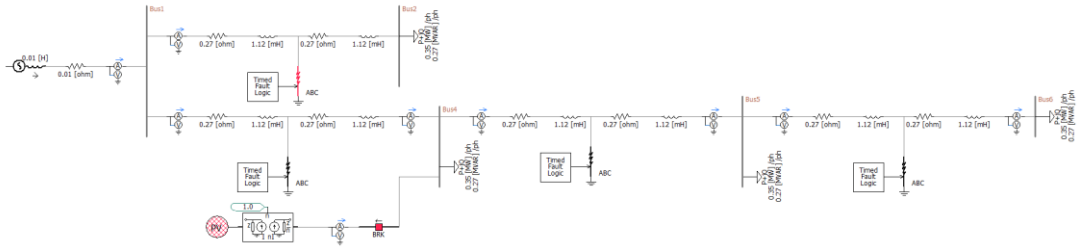

Fig. 8. Simulation model of distribution network in PSCAD.

Fig. 9 shows the current waveform of an external fault *f*3, where fault type is two-phase fault, the angle difference is 90° caused by the asynchronous problem, the fault occurrence time is 1s, the load level is 0.35kW+j0.27kVAr and the transition resistance is 15Ω. The similarity value of the PSCFCs is 1.8316, resulting the protection disoperation. The process of the self-synchronization technology is detailed as follows for this case of external fault.

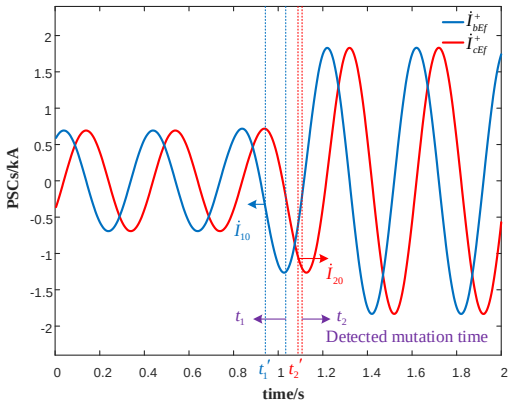

Fig. 9. Current waveform at fault point *f*3.

The detected current mutation times of PSCs at both ends of the line are 1.017s and 1.12s and are denoted by t_1 and t_2 respectively. According to the PSC self-synchronization technology, the differential current amplitudes $\left|\dot{I}_{10}-\dot{I}_2\right|$ are calculated, where $\dot{I}_{10}$ is the current phasor at time 0.95s for the head of the line and $\dot{I}_2$ represents any current phasor at the end of the line of 4 cycles before the time t_2. Fig. 10 has shown the changes of the differential current amplitudes $\left|\dot{I}_{10}-\dot{I}_2\right|$. According to Fig. 9 and Fig. 10, the time 1.1096s closest to the time t_2 is preliminarily determined as the synchronization point of time 0.95s and is denoted by t_2'. The current phasor $\dot{I}_2$ at the time t_2' is defined as $\dot{I}_{20}$.

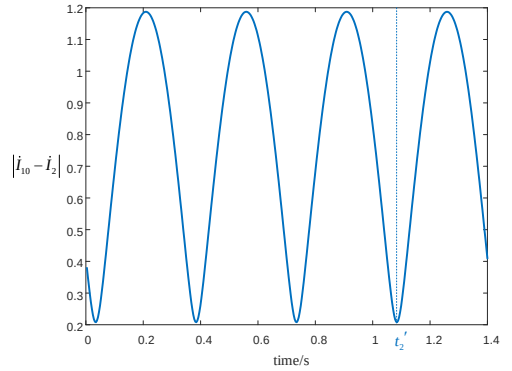

Fig. 10. Differential current amplitude between two ends of line at different time.

Next, the differential current amplitudes $\left|\dot{I}_1 - \dot{I}_{20}\right|$ are calculated, where $\dot{I}_1$ represents any current phasor at the head of the line between the time t_1 and the time 0.95s. The time corresponding to the minimum are 0.97s, 0.99s and 1.01s, where 1.01s is closest to the time t_1. Therefore, $\dot{I}_{10}$ at the time 1.1096s is synchronized with $\dot{I}_{20}$ at the time 1.01s. The angle difference 89.91° caused by the asynchronous problem is calculated to realize the self-synchronization technology of PSCs. After implementing the self-synchronization technology, the similarity value of PSCFCs is 2.52×10^{-5} by the formula 6. In contrast, it is 1.8316 before implementing the self-synchronization technology. Therefore, the proposed self-synchronization technology can effectively solve the asynchronous problem. Furthermore, the protection principle can identify this external fault case correctly. Similarly, Fig. 11 shows the current waveform of an internal fault *f*2, where fault type is two-phase fault, the angle difference is 90° caused by the asynchronous problem, the fault occurrence time is 1s, the load level is 0.35kW+j0.27kVARs and the transition resistance is 15Ω.

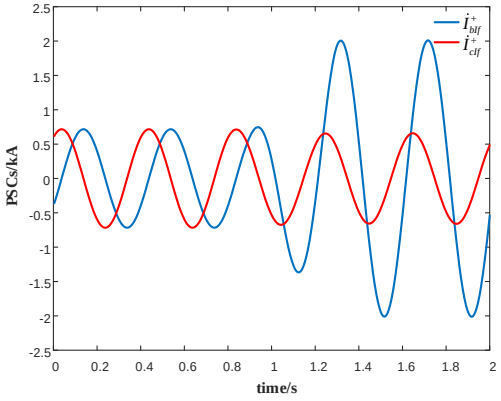

Fig. 11. Current waveform at fault point *f*2.

After implementing the self-synchronization technology, the similarity value of the PSCFCs is 2.1501 by the formula 6. In contrast, it is 1.2786 before implementing the self-synchronization technology. In this case, the protection principle can accurately identify fault before and after implementing the self-synchronization. In fact, due to the combined effect of asynchronous problem and fault current, the amplitudes and the phase angles of PSCs in case of internal faults are similar under the certain fault conditions, resulting in the refusal-operation of protection. However, the proposed self-synchronization technology can effectively solve this problem.

Considering various fault conditions, many simulations are conducted to verify the proposed protection with the proposed self-synchronization, where the results are summarized in Tables 1-5. According to Tables 1-3, the similarity

values of PSCFCs for external faults are higher than the protection threshold due to the asynchronous problem, which can cause protection disoperation. But after implementing the self-synchronization technology, the similarity values of the PSCFCs meet $D(\Delta\dot{I}_1, \Delta\dot{I}_2) < D_{set}$ and the protection can reliably identify these external faults. Similarly, according to Tables 4-5, the similarity values of PSCFCs in event of internal fault meet $D(\Delta\dot{I}_1, \Delta\dot{I}_2) > D_{set}$, the protection can accurately identify these faults. The results show that the protection with the self-synchronization technology can accurately identify external and internal faults under different fault conditions. Different transition resistances in event of internal and external faults are conducted to verify the ability of the proposed protection against the transition resistance, where the results are summarized in Tables 2 and 5. According to Table 2, after implementing the self-synchronization technology, the similarity values of PSCFCs meet $D(\Delta\dot{I}_1, \Delta\dot{I}_2) < D_{set}$ under higher transition resistance and the protection can reliably identify these external faults. Similarly, according to Table 6, the similarity of PSCFCs in event of internal faults meet $D(\Delta\dot{I}_1, \Delta\dot{I}_2) > D_{set}$ under higher transition resistance, the protection can reliably identify these internal faults.

In summary, the simulation results show that the protection principle proposed in this paper can accurately identify the interphase faults under different fault conditions and has ability against the transition resistance.

Table 1

Simulation results of external faults with different DG penetration

			Before implementing the self-synchronization			After implementing the self-synchronization		
DG penetration	Fault type	D_{set}	Angle difference	$D(\Delta\dot{I}_1, \Delta\dot{I}_2)$	Result of identification	Angle difference	$D(\Delta\dot{I}_1, \Delta\dot{I}_2)$	Result of identification
35%	Two-phase short-circuit	0.1	14.4°	0.2695	Internal fault	0.003°	3.2708×10^{-5}	External fault
	Three-phase short-circuit	0.1	10.8°	0.4969	Internal fault	0.004°	8.4152×10^{-5}	External fault
40%	Two-phase short-circuit	0.1	14.4°	0.2667	Internal fault	0.006°	3.2209×10^{-5}	External fault
	Three-phase short-circuit	0.1	18°	0.8235	Internal fault	0.01°	8.3753×10^{-5}	External fault
50%	Two-phase short-circuit	0.1	10.8°	0.2022	Internal fault	0.002°	3.2610×10^{-5}	External fault
	Three-phase short-circuit	0.1	14.4°	0.6584	Internal fault	0.004°	8.4072×10^{-5}	External fault

Table 2

Simulation results of external fault with different transition resistance

			Before implementing the self-synchronization			After implementing the self-synchronization		
Transition resistance[Ω]	Fault type	D_{set}	Angle difference	$D(\Delta\dot{I}_1, \Delta\dot{I}_2)$	Result of identification	Angle difference	$D(\Delta\dot{I}_1, \Delta\dot{I}_2)$	Result of identification
15	Two-phase short-circuit	0.1	21.6°	0.5031	Internal fault	0.015°	3.8738×10^{-5}	External fault
	Three-phase short-circuit	0.1	14.4°	0.6083	Internal fault	0.003°	1.0359×10^{-5}	External fault
30	Two-phase short-circuit	0.1	10.8°	0.1576	Internal fault	0.005°	2.1157×10^{-5}	External fault
	Three-phase short-circuit	0.1	36°	1.3141	Internal fault	0.03°	6.0931×10^{-5}	External fault
50	Two-phase short-circuit	0.1	28.8°	0.2837	Internal fault	0.023°	1.3190×10^{-5}	External fault
	Three-phase short-circuit	0.1	18°	0.4513	Internal fault	0.013°	3.8681×10^{-5}	External fault

Table 3

Simulation results of external faults with different fault occurrence time

			Before implementing the self-synchronization			After implementing the self-synchronization		
Fault occurrence time[s]	Fault type	D_{set}	Angle difference	$D(\Delta\dot{I}_1, \Delta\dot{I}_2)$	Result of identification	Angle difference	$D(\Delta\dot{I}_1, \Delta\dot{I}_2)$	Result of identification
1.0	Two-phase short-circuit	0.1	28.8°	0.6275	Internal fault	0.025°	3.0350×10^{-5}	External fault
	Three-phase short-circuit	0.1	18°	0.8266	Internal fault	0.012°	8.2502×10^{-5}	External fault
1.01	Two-phase short-circuit	0.1	10.8°	0.2037	Internal fault	0.005°	3.0397×10^{-5}	External fault
	Three-phase short-circuit	0.1	36°	1.6399	Internal fault	0.032°	8.2797×10^{-5}	External fault
1.02	Two-phase short-circuit	0.1	21.6°	0.4095	Internal fault	0.013°	3.0100×10^{-5}	External fault
	Three-phase short-circuit	0.1	43.2°	1.9677	Internal fault	0.046°	8.3936×10^{-5}	External fault

Table 4

Simulation results of internal faults at different fault location

			Before implementing the self-synchronization			After implementing the self-synchronization		
Fault location	Fault type	D_{set}	Angle difference	$D(\Delta\dot{I}_1, \Delta\dot{I}_2)$	Result of identification	Angle difference	$D(\Delta\dot{I}_1, \Delta\dot{I}_2)$	Result of identification
5%	Two-phase short-circuit	0.1	36°	1.1340	Internal fault	0.03°	1.1225	Internal fault

	Three-phase short-circuit	0.1	28.8°	3.0898	Internal fault	0.026°	2.9460	Internal fault
50%	Two-phase short-circuit	0.1	43.2°	1.1064	Internal fault	0.048°	1.0888	Internal fault
	Three-phase short-circuit	0.1	18°	2.9565	Internal fault	0.015°	2.8148	Internal fault
95%	Two-phase short-circuit	0.1	10.8°	1.0593	Internal fault	0.004°	1.0571	Internal fault
	Three-phase short-circuit	0.1	21.6°	2.8324	Internal fault	0.015°	2.6943	Internal fault

Table 5

Simulation results of internal faults at different load level

			Before implementing the self-synchronization			After implementing the self-synchronization		
Load level	Fault type	D_{set}	Angle difference	$D(\Delta\dot{I}_1, \Delta\dot{I}_2)$	Result of identification	Angle difference	$D(\Delta\dot{I}_1, \Delta\dot{I}_2)$	Result of identification
0.15kW+j0.07kVAr	Two-phase short-circuit	0.1	14.4°	1.0757	Internal fault	0.003°	1.0788	Internal fault
	Three-phase short-circuit	0.1	54°	2.9235	Internal fault	0.062°	2.7928	Internal fault
0.25kW+j0.17kVAr	Two-phase short-circuit	0.1	21.6°	1.0140	Internal fault	0.017°	1.0507	Internal fault
	Three-phase short-circuit	0.1	18°	2.8181	Internal fault	0.014°	2.7321	Internal fault
0.35kW+j0.27kVAr	Two-phase short-circuit	0.1	10.8°	0.9842	Internal fault	0.005°	1.0273	Internal fault
	Three-phase short-circuit	0.1	43.2°	2.6888	Internal fault	0.049°	2.6819	Internal fault

Table 6

Simulation results of internal faults with different transition resistance

			Before implementing the self-synchronization			After implementing the self-synchronization		
Transition resistance[Ω]	Fault type	D_{set}	Angle difference	$D(\Delta\dot{I}_1, \Delta\dot{I}_2)$	Result of identification	Angle difference	$D(\Delta\dot{I}_1, \Delta\dot{I}_2)$	Result of identification
15	Two-phase short-circuit	0.1	21.6°	1.3648	Internal fault	0.017°	1.3617	Internal fault
	Three-phase short-circuit	0.1	14.4°	3.5474	Internal fault	0.004°	3.3531	Internal fault
30	Two-phase short-circuit	0.1	10.8°	0.7719	Internal fault	0.006°	0.7724	Internal fault
	Three-phase short-circuit	0.1	36°	2.1823	Internal fault	0.032°	2.1501	Internal fault
50	Two-phase short-circuit	0.1	28.8°	0.3498	Internal fault	0.027°	0.4847	Internal fault

	Three-phase short-circuit	0.1	18°	1.4041	Internal fault	0.015°	2.1501	Internal fault

6. Conclusions

To improve the protection performance for the active distribution network, a pilot protection based on a new PSC self-synchronization technology is proposed in this paper, where the similarity of PSCs at both ends of the line is used to identify the external fault and the internal fault. The proposed self-synchronization technology calculates the angle difference caused by the asynchronous problem through minimizing the amplitude of the differential current before the fault occurrence. According to the calculated angle difference, the synchronization of the PSCs is realized. Further, the similarity value of the PSCFCs is calculated to distinguish the external fault and the internal fault.

The theoretical analysis and simulation results show that the similarity value of PSCFCs is lower when an external fault occurs. While the similarity value is higher when an internal fault occurs. The proposed pilot protection shows good performances under various fault conditions, such as DG penetration, fault type, fault occurrence time, load level and other factors. In particular, the protection has a certain ability against the transition resistance. Therefore, with the development of DG, the protection principle proposed in this paper has a good application prospect.

Acknowledgement

This work was supported by the Science and Technology Project of State Grid Corporation of China (SGLNBX00HLJS2200485).

R E F E R E N C E S

[1]. T. Vishnuvardhan, P. Janmejava, A. Anubha, S. Manohar and S. S. Garudachar. Protection challenges under bulk penetration of renewable energy resources in power systems: a review. CSEE J Power Energy Syst. 2017, **3**: 365-379.

[2]. P. T. Manditereza, R. C. Bansal. Fault detection and location algorithm for DG-integrated distribution systems. J. Eng. 2018, 1286-1290.

[3]. K. Pereira, B.R. Pereira, J. Contreras, J.R.S. Mantovani. A multiobjective optimization technique to develop protection systems of distribution networks with distributed generation. IEEE Trans Power Syst. 2018, **33**: 7064-7075.

[4]. P. T. Manditereza, R. C. Bansal. Review of technical issues influencing the decoupling of DG converter design from the distribution system protection strategy. IET Renew Power Gener. 2018, **12**: 1091-1100.

[5]. K. Moses, M. Yateendra, V Mahinda. Morphological fault detector for adaptive overcurrent protection in distribution networks with increasing photovoltaic penetration. IEEE Trans Sustain Energy. 2018, **9**: 1021-1029.

[6]. V.A. Papaspiliotopoulos, G.N. Korres, V.A. Kleftakis, N.D. Hatziargyriou. Hardware-in-the-loop design and optimal setting of adaptive protection schemes for distribution systems with distributed generation. IEEE Trans Power Deliv. 2017, **32**: 393-400.

[7]. N.E. Naily, S.M. Saad, A. Elhaffar, T. Hussein, F.A. Mohamed. Mitigating the impact of distributed generator on medium distribution network by adaptive protection scheme. Int Renew Energy Cong 2017: 1-6.

[8]. H. Mohammed A, I. Machesh S. The influence of inverter-based DGs and their controllers on distribution network protection. IEEE Trans Ind Appl 2014, **50(4)**: 2928–37.

[9]. L.M. Pintos, M. Moreto, J.G. Rolim. Applicability analysis of directional overcurrent relay without voltage reference in microgrids. IEEE Latin America Trans 2016, **14(2)**: 687–93.

[10]. J.L. Sun, Y.L. Li, S.W. Li, et al. A fast current protection scheme for distribution system with distributed generations. Journal of Tianjin University. 2010, **43(2)**, 102-108(in Chinese).

[11]. S. Elmer, G Naren. Summary of useful concepts about the coordination of directional overcurrent protections. CSEE J Power Energy Syst 2019, **5(3)**:382–90.

[12]. W. Q. Li, Li, S. H., ang, Shang Shangxing.; et al. An adaptive distance protection scheme for distribution system with distributed generation. Electric Power Engineering. 2012, **28(9)**, 1-4(in Chinese).

[13]. H.L. Gao, J. Li, B.Y. Xu. Principle and implementation of current differential protection in distribution networks with high Penetration of DGs. IEEE Transactions on Power Delivery. 2017, **32(1)**, 565-574.

[14]. S. Xu, Y. Lu. Current amplitude differential protection for distribution system with DG. Trans China Electrotech Soc 2015, **30(18)**: 164-70.

[15]. X.W. Liu, Y.L. Li, X.L. Chen, et al. An improved scheme of longitudinal differential protection for teed lines with inverter-based distributed generations. Power System Technology. 2016, **40(4)**, 1257-1264(in Chinese).

[16]. B.W. Han, G. Wang, H.F. Li, et al. Novel pilot protection scheme for distribution networks with inverter-interfaced distributed generators. High Voltage Engineering. 2017, **43(10)**, 3453-3462(in Chinese).

[17]. H. J. Han, L.H. Mu, F. Zhang, et al. Microgrid protection considering low voltage ride-through of IIDG. Proceedings of the CSEE. 2017, 37(1), 110-119(in Chinese).

[18]. Z. S. Fariborz, M. Parniani. A comprehensive digital protection scheme for low-voltage microgrids with inverter-based and conventional distributed generations. IEEE Trans Power Delivery 2017, **32(1)**: 441–52.

[19]. G.Q. Pan, D.H. Zeng, G. Wang, et al. Fault analysis on distribution network with inverter interfaced distributed generations based on PQ control strategy. Proceedings of the CSEE. 2014, **34(4)**, 555-561(in Chinese).

[20]. J. Li, H.L. Gao, G.F. Zhu. Inverse-time current differential protection in active distribution network considering characteristics of inverter-interfaced distributed generations. Transactions of China Electrotechnical Society. 2016, **31(17)**, 74-83(in Chinese).

[21]. T.S. Bi, S.M. Liu, A.C. Xue, et al. Fault characteristics of inverter-interfaced renewable energy sources. Proceedings of the CSEE. 2013, **33(13)**, 165-171(in Chinese)